Journal of Applied Polymer Science

Modification of Ramie Fabric with a Metal-Ion-Doped Flame-Retardant Coating

Lili Wang,[1,2] Tao Zhang,[1,2] Hongqiang Yan,[1] Mao Peng,[2] Zhengping Fang[1,2]

[1]Laboratory of Polymer Materials and Engineering, Ningbo Institute of Technology, Zhejiang University, Ningbo 315100, China
[2]MOE Key Laboratory of Macromolecular Synthesis and Functionalization, Institute of Polymer Composites, Zhejiang University, Hangzhou 310027, China
Correspondence to: Z. Fang (E-mail: zpfang@zju.edu.cn)

ABSTRACT: Transition-metal-ion-doped flame-retardant coatings were constructed on the surface of ramie fabrics by a layer-by-layer (LbL) assembly technique to investigate possible cooperative actions that could improve the fabric's flame-retardant efficiency. We found that these functional coatings, consisting of poly(vinylphosphonic acid) (the anionic layer) and branched polyethylenimine/cupric or zinc ions (the cationic layer), improved the fire retardancy of the ramie fabrics remarkably. Attenuated total reflectance–Fourier transform infrared (FTIR) spectroscopy and energy dispersive X-ray spectroscopy demonstrated the successful LbL assembly process and the incorporation of metal ions into the coating. Thermogravimetric analysis coupled with FTIR spectrometry, vertical flame testing, and microscale combustion calorimetry confirmed the improved thermal stability and reduced flammability of the coated ramie fabrics. All of the results show that the metal-ion-doped flame-retardant coatings not only dramatically increased the residues but also retained the original weave structure and fiber morphology of ramie fabrics well. The enhanced flame-retardant efficiency may have been caused by the lower decomposition temperature of the flame-retardant coating, as promoted by cupric and zinc ions, and as a result, may have helped the flame-retardant activity to take place earlier. © 2013 Wiley Periodicals, Inc. J. Appl. Polym. Sci. 129: 2986–2997, 2013

KEYWORDS: coatings; fibers; flame retardance; properties and characterization; self-assembly

Received 20 August 2012; accepted 11 January 2013; published online 15 February 2013
DOI: 10.1002/app.39015

INTRODUCTION

Ever since the 1950s, lots of attention has been paid to the flame-retardant treatment of textiles that are ubiquitous in our daily life.[1] Plenty of modification methods and flame retardants have been applied to limit the flammability of synthesized and natural fibers. Continuously advancing science and technology are available for the development of more convenient methods and more effective flame retardants. Among various flame-retardant methods, the surface modification and functionalization of textiles is a widely used technique, which can retain the properties of the original substrate to the maximum extent. Furthermore, Decher and Hong[2] provided a new method [a.k.a., layer-by-layer (LbL) assembly] for fabricating functional thin films on the surface of multifarious substrates simply by the sequential irreversible adsorption of the positively charged polyelectrolyte (polycation) and negatively charged polyelectrolyte (polyanion). The electrostatic attraction between the alternatingly deposited polycation and polyanion holds them together and leads to the formation of an insoluble complex. Additionally, the properties of the assembled films are controllable through the adjustment of the molecular weight[3,4] and charge density[5] of polyelectrolyte, the pH[6] and temperature[7] of the deposition solution, and the deposition time.[8] Apart from electrostatic attraction, it has been demonstrated that hydrogen bonding,[9,10] covalent bonding,[11,12] and metal-ion coordination[13,14] can also be used as the driving force for assembly. Recently, it has been demonstrated that LbL assembly is an efficient way to construct flame-retardant coatings on textiles.[15–19]

Ramie fiber is one of the most abundant natural fibers. Because of its high intensity, fast moisture absorption, and good thermal conductivity, it is widely used for clothing and furnishing materials. It can also be used as reinforcements for polymer composites and so on.[20] As early as 1967, the United Kingdom enacted nightwear safety legislation to drive improvement in the fire-safety levels of girls' nightdresses.[21] As this directly concerns people's security of life, a great effort should be made to diminish potential fire hazards. The most commonly used flame retardants nowadays include halogen-, phosphorus-, and

Additional Supporting Information may be found in the online version of this article.

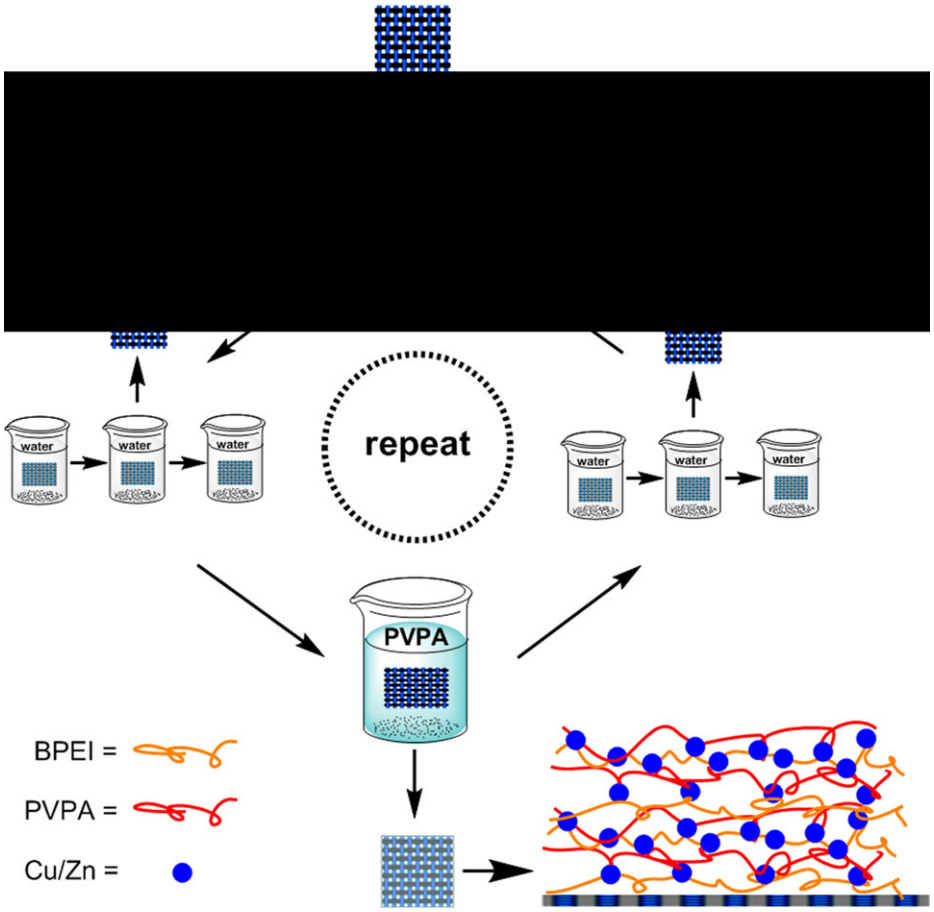

Scheme 1. Schematic representation of the LbL assembly. [Color figure can be viewed in the online issue, which is available at wileyonlinelibrary.com.]

nitrogen-containing compounds and inorganic flame retardants. However, despite their excellent flame retardance, some commonly used halogen-containing flame retardants were forbidden for use due to the dioxins they released, which were harmful to the human body and to the environment. Hence, phosphorus-based flame retardants are frequently used as alternatives. Additionally, phosphorus-based flame retardants have a high efficiency in their fire retardancy as they are effective in catalyzing the dehydration of fibers and charring to limit the spread of flammable gases.[22] Poly(vinylphosphonic acid) (PVPA) is a polymeric acid with as much as 33 wt % phosphorous content. The high phosphorous content makes PVPA a potential effective flame retardant. Unlike other insoluble polymers, the large amount of phosphonic acid groups give PVPA excellent water solubility, and its aqueous solution can be used as a polyanion component for LbL assembly. Moreover, its good biocompatibility makes PVPA friendly to the human body.[23]

It has been reported that some metal ions can enhance flame retardancy when worked together with phosphorus-based flame retardants.[24–26] These metal ions can promote the release of phosphoric acid from the phosphorus-containing compounds at lower temperatures and help flame-retardant activity to start earlier. Also, compounds of transition metals have been found to be good smoke suppressants;[27,28] these can also help improve the thermal stability of compounds. Some transition metals, such as zinc, are able for bacteriostasis.[29] Therefore, it was interesting to investigate whether the addition of transition-metal ions could further improve the flame-retardant abilities of a PVPA-containing flame retardant.

In this study, we prepared flame-retarding ramie fabrics that could be used to fabricate polymer composites for aircraft cabinet materials. Two transition-metal ions, namely, cupric and zinc ions, were doped into the LbL-assembled coating to evaluate the flame retardancy of these coatings on ramie fabrics. Here, PVPA served as the polyanion, and branched polyethylenimine (BPEI) served as the polycation. Metal ions were directly added to BPEI in their inorganic salt forms. Then, the alternate deposition of PVPA–metal-ion and BPEI–metal-ion aqueous solutions were conducted to fabricate coatings on the surface of the ramie fabrics. The LbL assembly processes were evaluated by attenuated total reflectance (ATR)–Fourier transform infrared (FTIR) spectroscopy and energy dispersive X-ray spectroscopy (EDX). The thermal stabilities of the ramie fabrics were measured by thermogravimetric analysis (TGA) and thermogravimetric analysis coupled with Fourier transform infrared spectrometry (TGA–FTIR). The flame-retardant behaviors were characterized by vertical flame testing (VFT) and microscale combustion calorimetry (MCC). The morphology of the coating and residues after VFT were studied by scanning electron microscopy (SEM).

Applied Polymer SCIENCE

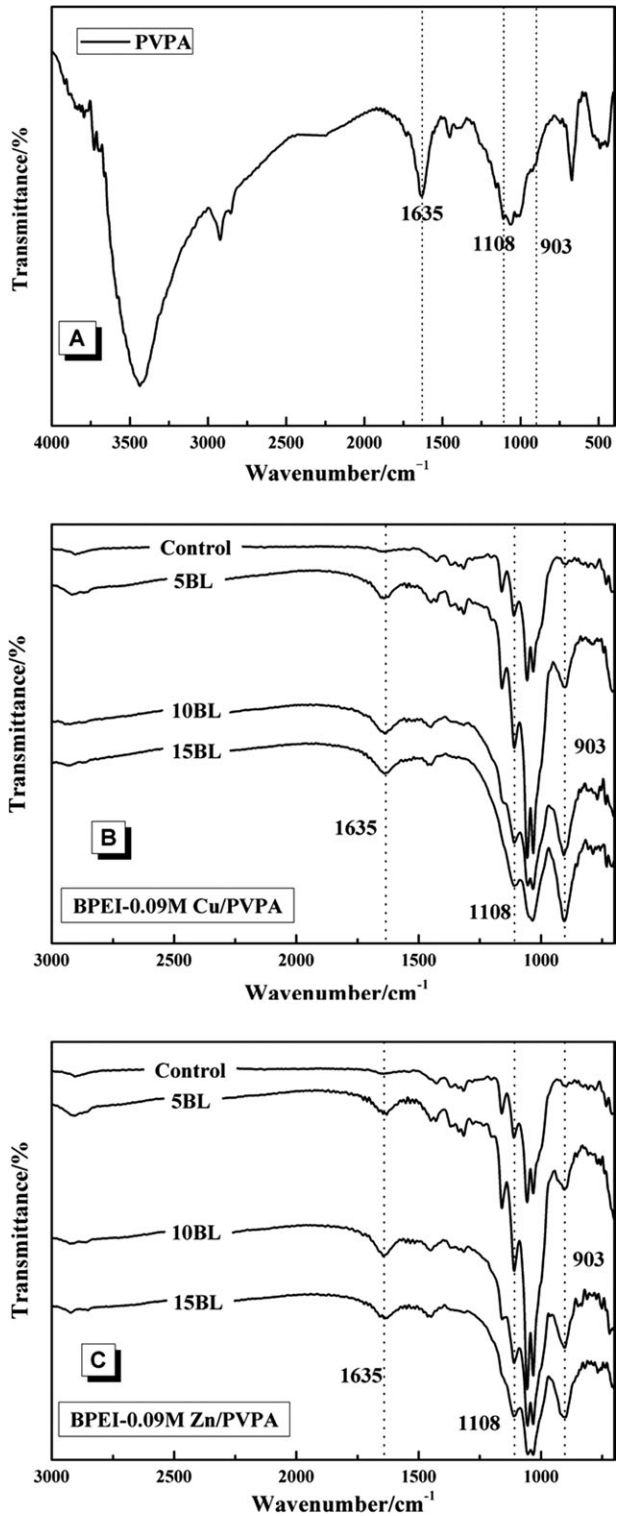

Figure 1. FTIR spectra of (A) PVPA, (B) ATR–FTIR spectra of the control and 0.09*M* Cu-coated fabrics, and (C) 0.09*M* Zn-coated fabrics.

EXPERIMENTAL

Materials

The ramie fabric (Jingzhu Fabric Industry Co., Ltd., Jiangxi, China) used as a deposition substrate was an orthogonal plain weave with approximately 50 threads/cm in both the warp and fill directions and a weight of 138 g/m^2; the fabric was washed with common detergent in water and dried for 2 h at 60°C.

Vinylphosphonic acid (TCI, Shanghai, China, 95% purity) was used for the synthesis of PVPA[30] (1.36×10^5 g/mol) to prepare 1 wt % deposition solutions with 18.2 Mω deionized water. Concentrations of 0.03 and 0.09*M* cupric sulfate anhydrous ($CuSO_4$; Jinshan Tingxin Chemical Reagent Factory, Shanghai, China) and zinc chloride ($ZnCl_2$; Sinopharm Chemical, Ltd., Shanghai, China) were added to 1 wt % BPEI solution (Aldrich, Milwaukee, WI, 25,000 g/mol). All of the reagents were used as received without further purification.

LbL Assembly

Four different coating recipes, 0.03 and 0.09*M* Cu^{2+} and 0.03 and 0.09*M* Zn^{2+}, were prepared manually. As shown in Scheme 1, the ramie fabrics were dipped sequentially into the BPEI–$CuSO_4$ or BPEI–$ZnCl_2$ and PVPA solutions for 5 min; this was followed by immersion in deionized water for 5 min and drying. Each BPEI–(Cu/Zn)/PVPA pair is referred to as a bilayer (BL). Five, ten, and fifteen BLs were built for each system. After the desired BL numbers were achieved, the coated fabrics were dried at 60°C for 2 h.

Characterization

The ATR–FTIR spectra were recorded with a Nicolet 6700 FTIR spectrometer (Thermo Fisher Scientific, Waltham, MA) equipped with an ATR device. The TGA–FTIR spectrometry was conducted by a TG 209 F1 thermogravimetric analyzer (Netzsch, Selb, Germany) that was interfaced to a Nicolet IS10 FTIR spectrophotometer (Thermo Fisher Scientific, Waltham, MA). All samples were approximately 10 mg and were kept at 100°C for 5 min first to remove absorbed moisture; they were then heated up to 600°C at a heating rate of 20°C/min in air. The VFTs were performed according to ASTM D 6413 with a horizontal and vertical flammability cabinet (model CZF-3, Nanjing Jiangning Analytical Instrument Factory, Nanjing, China). The afterflame times were recorded as the averages of five measurements for each sample. MCC tests were carried out on a Govmak MCC-2 microscale combustion calorimeter (Govmark, Farmingdale, NY). Samples weighing 4–5 mg were first kept at 100°C for 5 min to remove the adsorbed moisture and were then heated to 650°C at a heating rate of 1°C/s. The surface morphology of the uncoated and coated fabrics, the residual chars after the VFT, and the surface element contents of the coated fabrics were obtained with a Hitachi S-4800 field emission scanning electron microscope equipped with an energy dispersive X-ray spectrometer (Hitachi, Japan).

RESULTS AND DISCUSSION

Characterization of the LbL Coatings

Ellipsometry and quartz crystal microbalances are two commonly used methods to characterize the thickness and weight of LbL-assembled films. Both testing methods use one-dimensional substrates, such as silicon wafers, quartz slides, and Ti/Au crystals. In this study, the ramie fabric was a three-dimensional (3D) substrate. Therefore, the data obtained from ellipsometry or a quartz crystal microbalance could not represent the real coating on the fabric well. As a result, we investigated the thickness and weight of the LbL-assembled coatings directly from the coated fabric through ATR–FTIR spectroscopy and EDX.

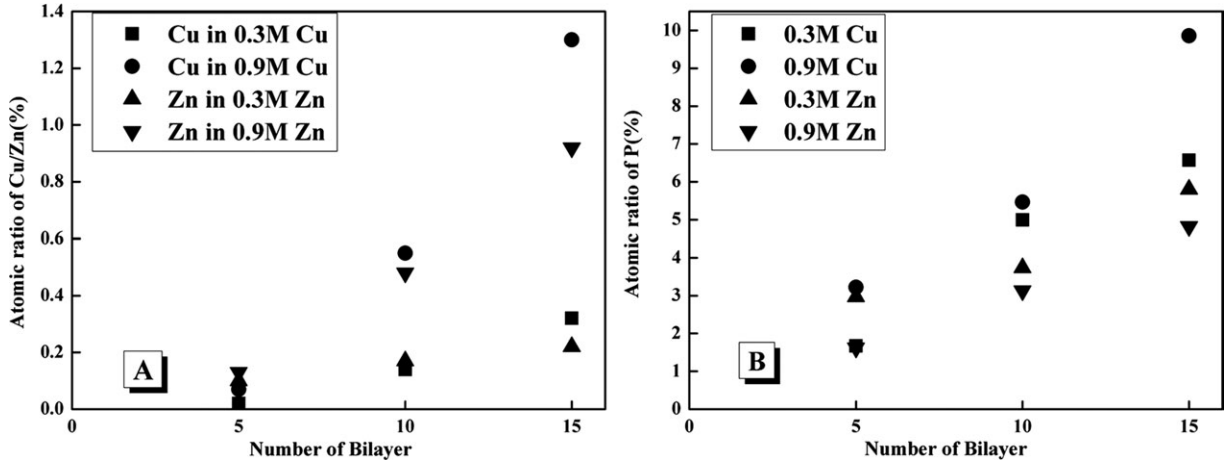

Figure 2. Relationship between the elemental contents of all of the coated ramie fabrics and the number of deposited layers.

Figure 1 shows the FTIR spectrum of PVPA and the ATR–FTIR spectra of the control and all of the 0.09*M* Cu/Zn-coated fabrics (see Figure S1 in the Supporting Information for the ATR–FTIR spectra of the 0.03*M* Cu/Zn-coated fabrics). The bands at wave numbers of 1635 cm^{-1} (bending vibrations of O—H in P—OH groups) and 1108 and 907 cm^{-1} (stretching vibrations of P—O

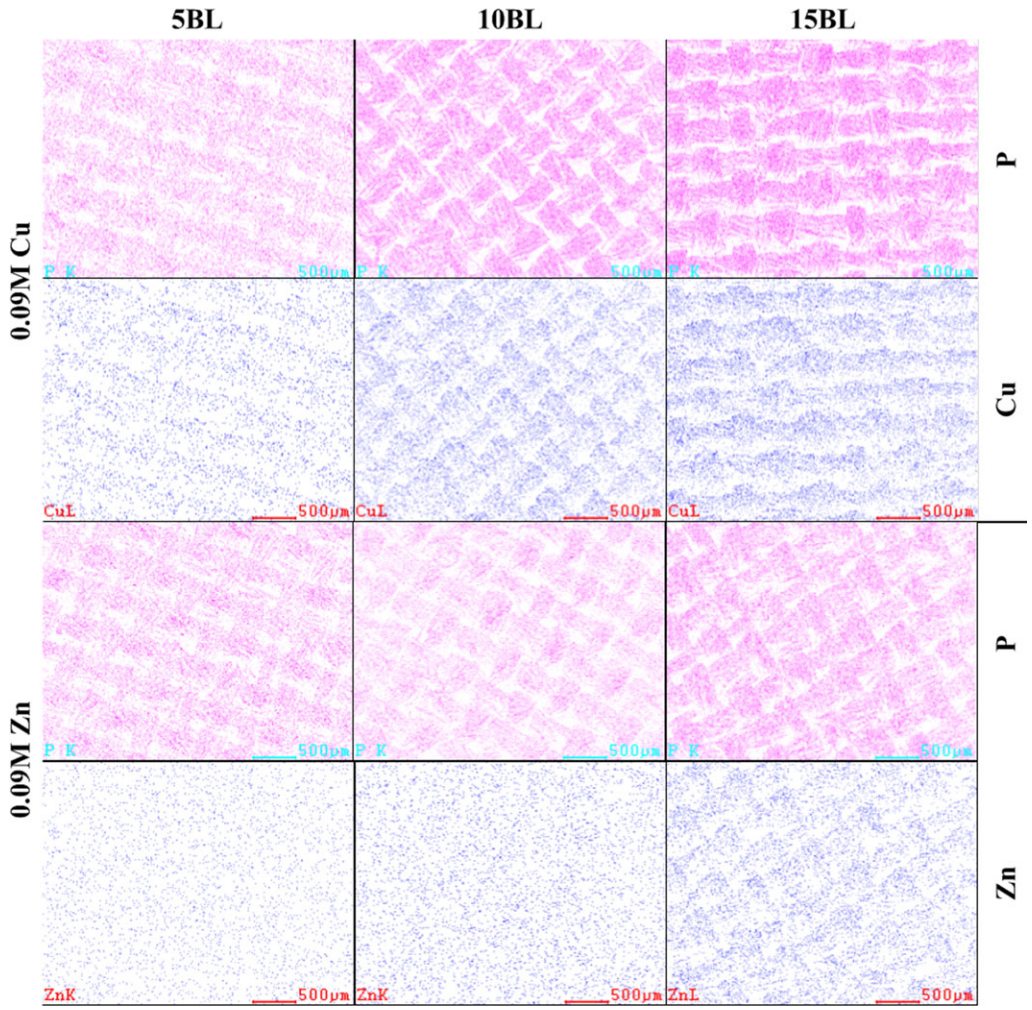

Figure 3. Elemental maps of all of the PVPA/BPEI–0.09*M* $CuSO_4$- and PVPA/BPEI–0.09*M* $ZnCl_2$-deposited coatings. [Color figure can be viewed in the online issue, which is available at wileyonlinelibrary.com.]

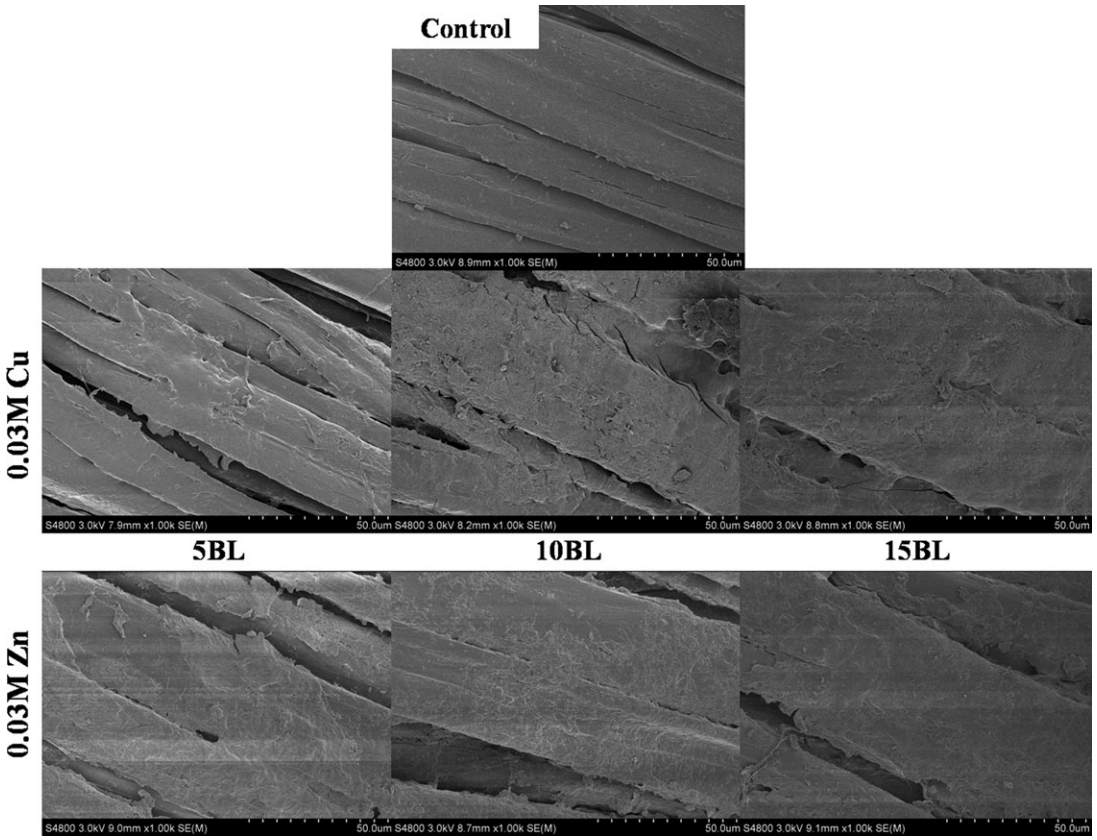

Figure 4. SEM images of the control and all of the PVPA/BPEI–0.03*M* $CuSO_4$- and PVPA/BPEI–0.03*M* $ZnCl_2$-coated ramie fabrics.

in P—OH groups)[31–33] in Figure 1(A) still appear in Figure 1(B,C); this indicates the presence of the PVPA-containing coating on the surface of the ramie fabric. With increasing number of deposited layers, the intensity of the three peaks got stronger; this confirmed a successful LbL construction process.

EDX was employed to qualitatively characterize the growing of the LbL-assembled coating on the ramie fabrics. There were four elements taken into account (viz., carbon, oxygen, phosphorous, and copper or zinc). The atomic ratios of phosphorous and the copper or zinc on the surface of the coated ramie fabrics are shown in Figure 2. For all of the coated fabrics, both the contents of P and Cu/Zn showed a linear increase as a function of the BL numbers; this further confirmed the successful fabrication of the LbL assembly coatings on the surface of the ramie fabrics and the incorporation of metal ions into the coatings. With higher concentration solutions, more Cu/Zn contents were found in the coatings with the same assembled BLs. What is more, a very uniform coverage of the coating on the surface

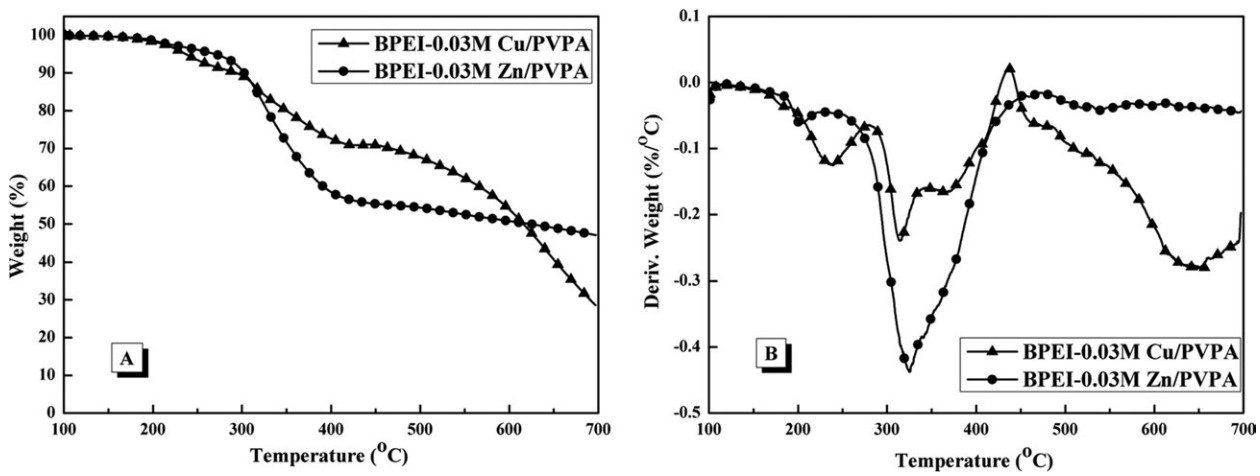

Figure 5. TGA and DTG curves of the 0.03*M* Cu- and Zn-doped BPEI and PVPA complexes.

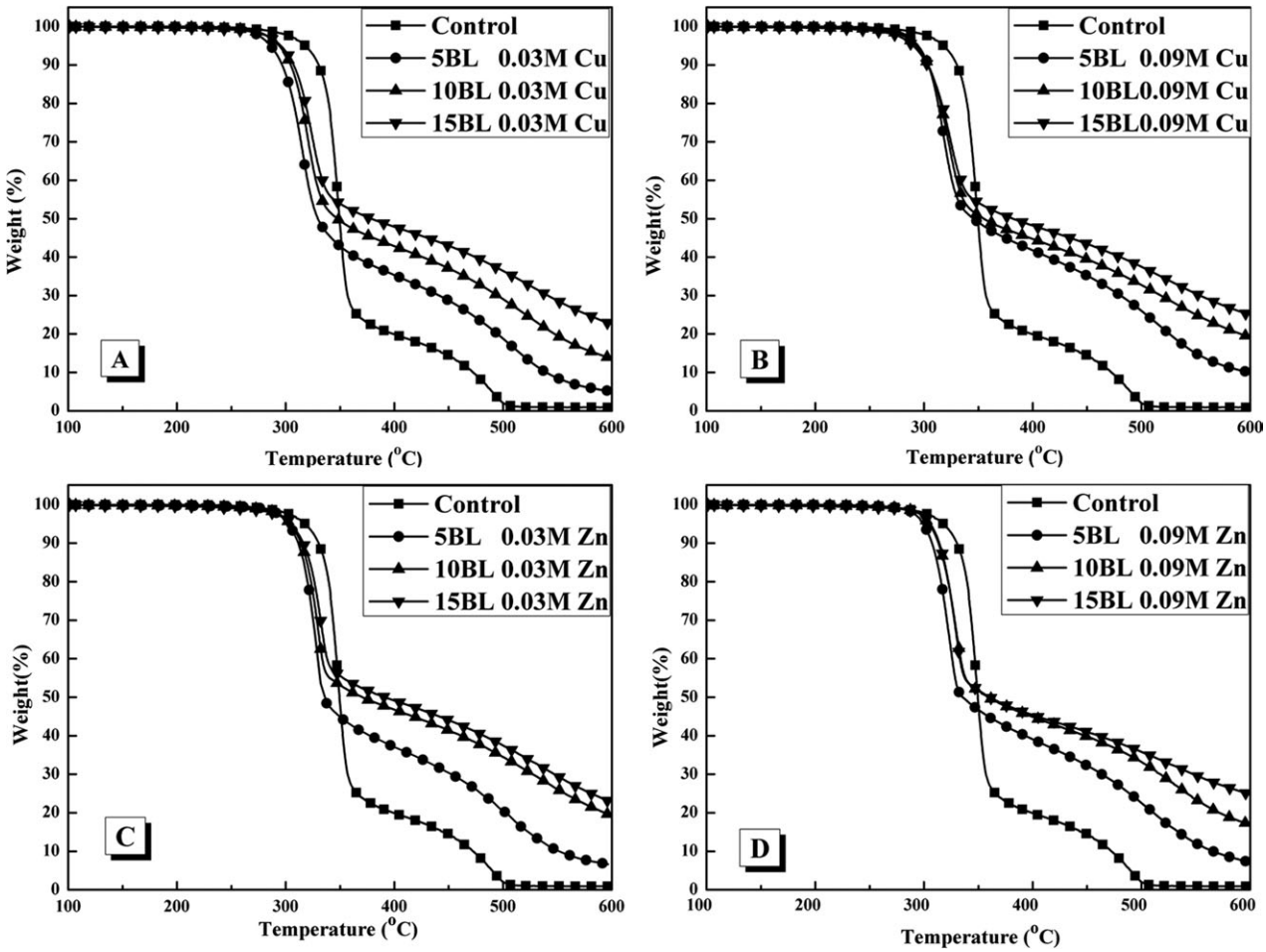

Figure 6. TGA curves of the control and all of the coated ramie fabrics.

of fabrics was achieved, as shown in Figure 3 for the element maps of the 0.09*M* Cu- and 0.09*M* Zn- coated fabrics; this was also observed in the 0.03*M* Cu- and 0.03*M* Zn-coated fabrics (see Figure S2 in the Supporting Information for the element maps of the 0.03*M* Cu- and 0.03*M* Zn-coated fabrics). It was clear that both P and Cu/Zn dispersed homogeneously in the coating, whose maps almost reproduced the morphology of the original fabric. The higher the number of assembled BLs was, the more accurate the maps showed the original morphology. Also, the color got darker with a greater number of depositions; this indicated that more coating was deposited. The EDX data showed good agreement with the previous ATR–FTIR results.

SEM was further carried out to examine the morphology of the fibers after LbL deposition. As shown in Figure 4, the surface of the fibers in the control ramie fabric was neat and smooth, although for both the Cu- and Zn-coated fabrics, there was a layer of rough, thick coating covering the fibers. The rough surface of the coating might have been caused by the addition of metal ions.[34] The interstices between the fibers were also filled with coating, especially in the 15-BL coated fabrics.

Thermal Stability

To better evaluate the influence of the coating on the thermal stability of the ramie fabric, TGA curves of the Cu- and Zn-doped BPEI and PVPA complexes were obtained, as shown in Figure 5. Both complexes decomposed earlier than 200°C and left more than 50 wt % residue at 600°C. Figure 5(B) shows that the Zn-doped BPEI and PVPA complex had two decomposition processes; the one around 325°C was the main decomposition step. The first decomposition of the Cu-doped BPEI and PVPA complex occurred earlier than in the Zn-doped complex, and the main decomposition happened at 314°C; this indicated a better catalytic effect of Cu on the degradation of the BPEI and PVPA complex.

Figure 6 shows the thermal degradation curves for all of the fabrics, and Table I summarizes the main degradation temperatures, the weight gained after LbL assembly, and the amount of residue at 600°C. As shown in Figure 6, there were two decomposition steps for the control fabric. The first one was the main decomposition stage, starting from 300 to 350°C, with a weight loss of nearly 80 wt %; this was caused by the dehydration and decomposition of cellulose.[35] As early as 500°C, the control fabric had already decomposed completely to leave less than 1 wt

Applied Polymer SCIENCE

Table I. TGA Data of the Complexes and the Control and Coated Fabrics

Sample	Add-on (wt %)	$T_{-5\%}$ (°C)	T_{max} (°C)	600°C residues (wt %)
BPEI-0.03*M* Cu/PVPA complex	—	237	314	53.8
BPEI-0.03*M* Zn/PVPA complex	—	270	325	50.8
Control	—	318	349	0.87
BPEI-0.03*M* Cu/PVPA				
5 BL	2.5	286	315	5.2
10 BL	8.6	294	320	13.9
15 BL	13.3	296	323	22.8
BPEI-0.09*M* Cu/PVPA				
5 BL	4.3	295	317	10.2
10 BL	9.2	293	322	19.5
15 BL	12.1	290	323	25.2
BPEI-0.03*M* Zn/PVPA				
5 BL	3.7	301	327	6.6
10 BL	9.3	304	330	19.6
15 BL	13.4	306	333	23.1
BPEI-0.09*M* Zn/PVPA				
5 BL	2.3	300	326	7.4
10 BL	5.3	305	328	17.2
15 BL	9.2	306	329	25.0

% residue at the end of test. For all of the coated fabrics, the initial degradation temperatures ($T_{-5\%}$'s) and the maximum degradation temperatures (T_{max}'s) shifted to lower ones compared to those of the control fabric. This was because the decomposition of the two metal-ion-doped coatings started much earlier than that of the pristine ramie fabric; the released phosphate groups promoted the charring of the underlying fabric, which led to the earlier initial decomposition of the coated fabrics.[24] Although the first decomposition process was the main one for the coated fabrics as well, the temperature range got much smaller, and more residue, as much as 50 wt %, was left. Moreover, all of the Cu/Zn-coated fabrics showed a significant increase in residues at 600°C; this showed that the Cu/Zn-doped coatings helped to improve the thermal stability of the underlying fabric at high temperatures.[36] We noted that the

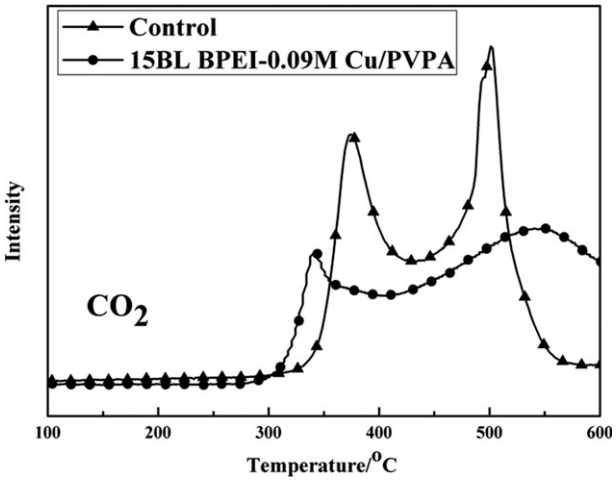

Figure 8. Adsorption intensity of CO_2 during degradation.

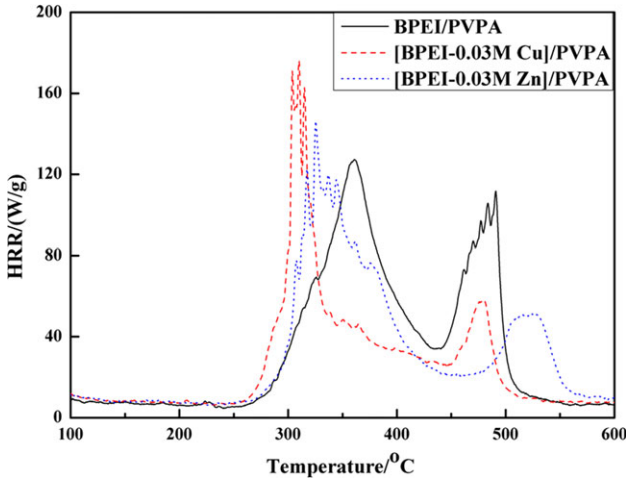

Figure 9. Heat release rate (HRR) curves of the complex. [Color figure can be viewed in the online issue, which is available at wileyonlinelibrary.com.]

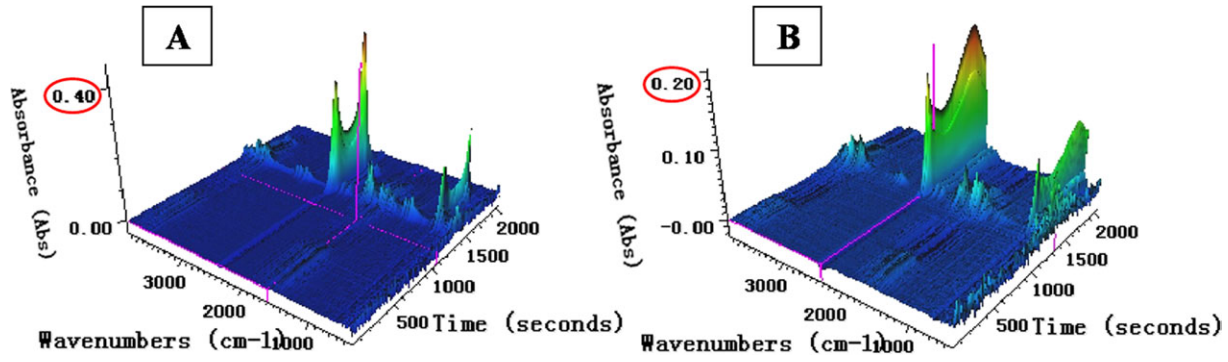

Figure 7. 3D surface graphs of the FTIR spectra of the evolved gases produced by the (A) control fabric and (B) 15-BL 0.09*M* Cu-coated fabric. [Color figure can be viewed in the online issue, which is available at wileyonlinelibrary.com.]

Table II. MCC Data of the Complex

Sample	HRC ($J\ g^{-1}\cdot K^{-1}$)	THR (kJ/g)	T_p (°C)	PHRR (W/g)	Residue (%)
BPEI/PVPA	120	13.0	358.3	118.5	30.5
BPEI-0.03*M* Cu/PVPA	181	11.5	303.7	168.2	42.0
BPEI-0.03*M* Zn/PVPA	138	10.8	324.6	139.4	40.0

residues of all of the coated fabrics were nearly twice as large as that of the coating. With higher deposition layer numbers, more residues were obtained; this revealed the good char promotion ability of the Cu/Zn-doped coatings. Additionally, when we compared al of the 15-BL coated fabrics, the fabrics doped with a higher metal-ion-concentration solutions resulted in more residues, whereas all of the 15-BL 0.09*M* Cu/Zn-coated fabrics gained less weight after deposition than the 15-BL 0.03*M* Cu/Zn-coated fabrics. All of the Cu-coated fabrics showed lower $T_{-5\%}$ and T_{max} values than the Zn-coated fabrics; this indicated a better catalytic effect of the Cu-doped coatings on the degradation of the ramie fabrics.

Volatile Products of the Ramie Fabrics during Degradation

To better understand the influence of the coating on the thermal degradation of the fabric, TGA–FTIR spectroscopy was conducted to identify the evolved gases produced during the TGA test. Figure 7 presents the 3D FTIR spectra of the virgin and 15-BL 0.09*M* Cu-coated fabrics. We found that the main products evolved during the degradation of both ramie samples were H_2O (3400–4000 cm^{-1}), CO_2 (2240–2400 cm^{-1}), and CO (2140–2235 cm^{-1}). Compared to the virgin fabric, the intensities of all of the adsorption peaks in the 15-BL 0.09*M* Cu-coated fabric were greatly reduced. Because the decomposition of the coating occurred earlier than in the underlying fabric, the released phosphate groups promoted the charring of the underlying ramie fabric, which prevented further decomposition of the ramie. According to Wilkie's et al.'s[37] study, water and ethylene are the two major products from the decomposition of PVPA. As for BPEI, the main degradation products are ammonia, ethylamine, pyrrhol, and C-substituted ethylpyrrholes.[38] Therefore, CO_2 is mainly induced by the degradation of fiber.

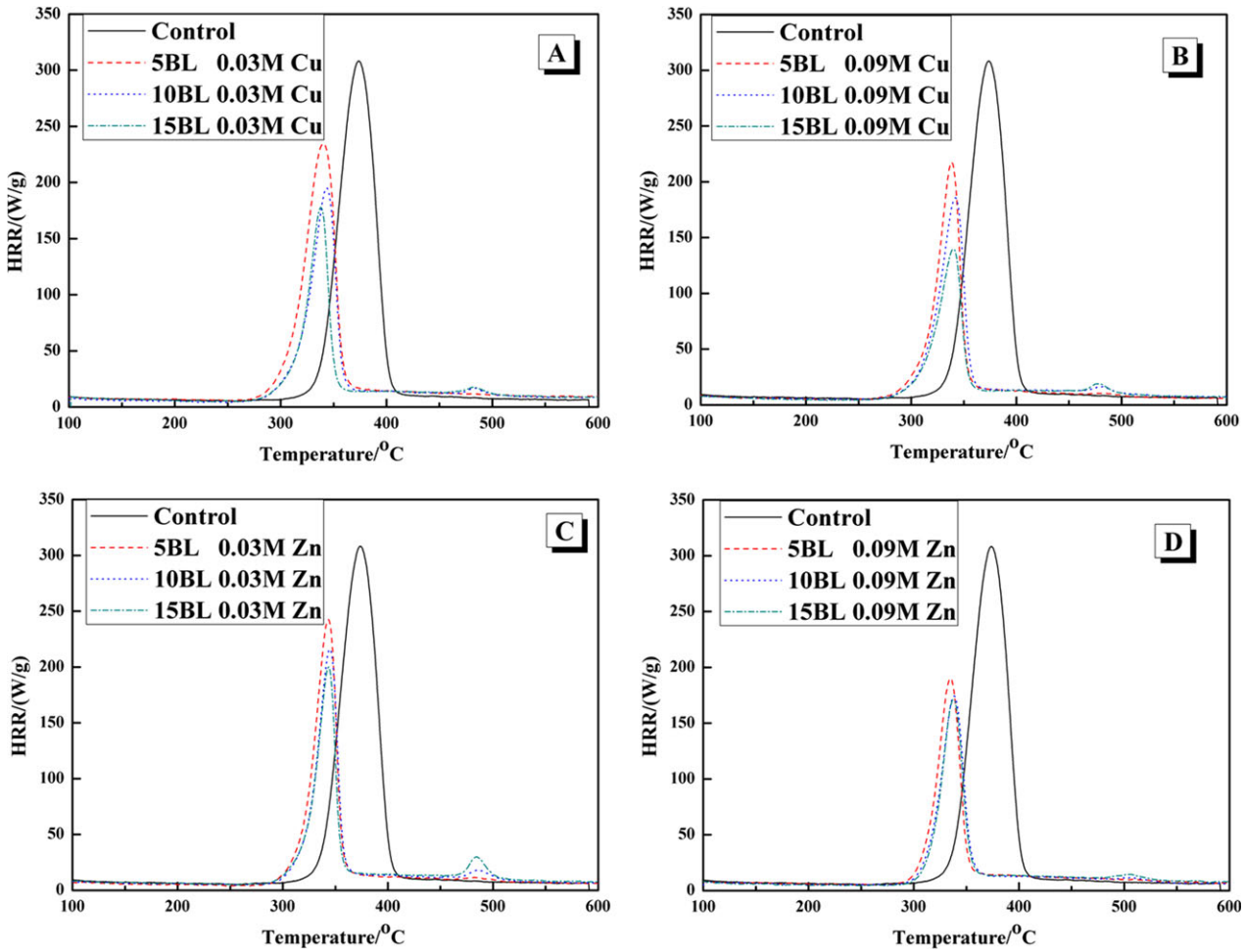

Figure 10. Heat release rate (HRR) curves of the control and all of the coated ramie fabrics. [Color figure can be viewed in the online issue, which is available at wileyonlinelibrary.com.]

Applied Polymer SCIENCE

Table III. MCC Data of the Control and All of the Coated Fabrics

Sample	HRC ($J\ g^{-1}\cdot K^{-1}$)	THR (kJ/g)	T_p (°C)	PHRR (W/g)	Residue (%)
Control	309	13.3	371.8	308.2	6.5
BPEI-0.03*M* Cu/PVPA					
5 BL	202	6.7	335.3	203.9	21.8
10 BL	192	5.7	340.5	191.8	25.0
15 BL	170	4.7	342.7	170.8	29.6
BPEI-0.09*M* Cu/PVPA					
5 BL	210	6.1	338.1	210.3	22.3
10 BL	178	5.8	342.0	178.2	25.2
15 BL	133	4.5	340.2	132.8	32.4
BPEI-0.03*M* Zn/PVPA					
5 BL	234	6.6	343.1	235.7	21.9
10 BL	209	5.9	344.8	209.1	25.4
15 BL	191	5.4	343.6	192.1	29.1
BPEI-0.09*M* Zn/PVPA					
5 BL	183	5.3	334.4	182.7	25.5
10 BL	167	5	338.3	167.1	27.1
15 BL	164	4.5	337.5	163.1	30.2

As shown in Figure 8 for the absorbance of CO_2 (the characteristic peak was at 2349 cm^{-1}) versus temperature, the evolution of CO_2 in the 15-BL 0.09*M* Cu-coated fabric happened at a lower temperature and ended up at a higher one compared to that of the control, whereas the intensity of CO_2 in the coated fabric was much lower than that of the control; this indicated a much slower release rate of CO_2 during the degradation of the 15-BL 0.09*M* Cu-coated fabric than that of the control. This also meant a much slower degradation speed of the coated fabric.

Flame-Retardant Properties

As a convenient method for estimating the combustion properties of polymer materials, MCC was used to investigate the key fire parameters of the ramie fabrics, including the temperature at maximum heat release rate (T_p), peak heat release rate (PHRR in W/g), total heat release (THR in kJ/g), and maximum heat release capacity (HRC; $J\cdot g^{-1}\cdot K^{-1}$). To better understand the effects of the two metal ions on the combustion behavior of the flame-retardant coatings, the combustion properties of their complexes with PVPA and BPEI were evaluated through MCC first. As shown in Figure 9 and Table II, both Cu and Zn helped to accelerate the decomposition of the original

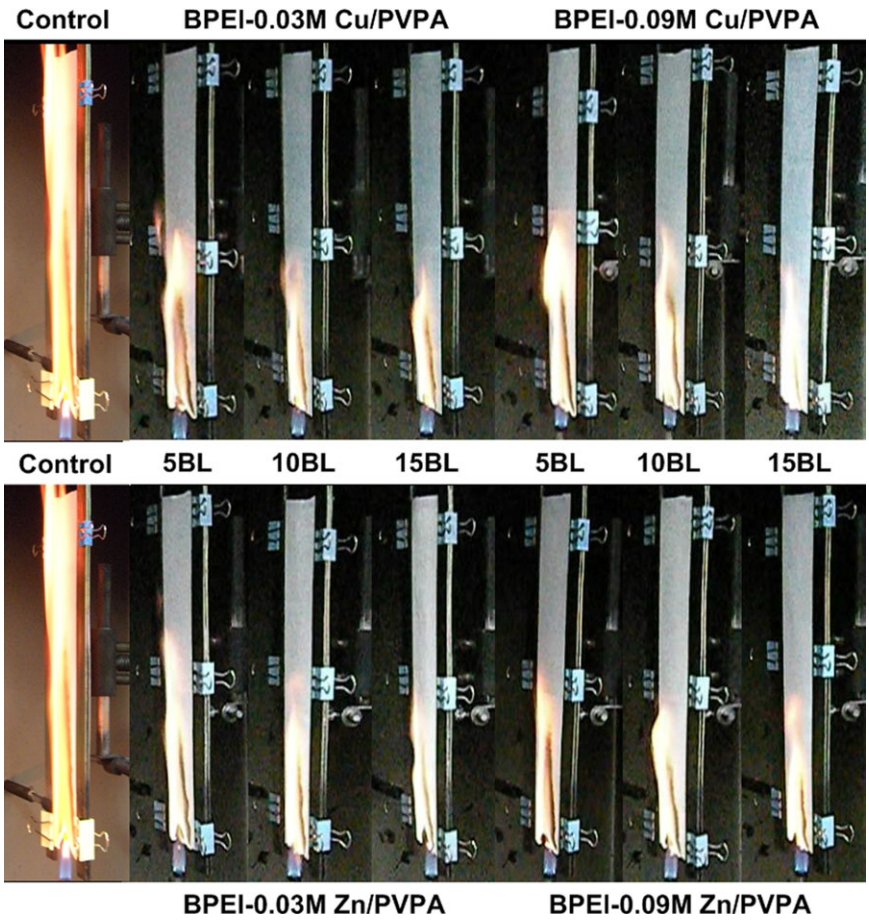

Figure 11. Images of all of the fabrics at 5 s after ignition during the VFT. [Color figure can be viewed in the online issue, which is available at wileyonlinelibrary.com.]

Table IV. Afterflame Time of the Control and All of the Coated Fabrics

Sample	Afterflame time (s)
Control	16.84 ± 2.14
5-BL BPEI-0.03*M* Cu/PVPA	11.85 ± 0.47
10-BL BPEI-0.03*M* Cu/PVPA	8.90 ± 0.31
15-BL BPEI-0.03*M* Cu/PVPA	7.88 ± 0.23
5-BL BPEI-0.09*M* Cu/PVPA	11.28 ± 1.48
10-BL BPEI-0.09*M* Cu/PVPA	7.97 ± 0.45
15-BL BPEI-0.09*M* Cu/PVPA	7.43 ± 0.09
5-BL BPEI-0.03*M* Zn/PVPA	9.80 ± 0.16
10-BL BPEI-0.03*M* Zn/PVPA	7.56 ± 0.54
15-BL BPEI-0.03*M* Zn/PVPA	7.23 ± 0.34
5-BL BPEI-0.09*M* Zn/PVPA	12.10 ± 0.13
10-BL BPEI-0.09*M* Zn/PVPA	7.03 ± 0.25
15-BL BPEI-0.09*M* Zn/PVPA	6.78 ± 0.12

BPEI/PVPA complex at lower temperatures and reduced the THR.

Figure 10 and Table III show the results of the control and all coated fabrics obtained from MCC. All of the coated fabrics had much lower THR and HRC values compared to the virgin fabric, and further reductions occurred with increasing BL numbers. The maximum reductions for THR and HRC were 66 and 57%, respectively. Additionally, this coincided with the TGA data; the residues of all of the coated fabrics increased remarkably from 6.5 to 32.4 wt %; this was also greater than that reported for flame-retardant cotton fabrics with an almost 17.6 wt % coating.[17] The greater amount of residues should have been caused by the addition of metal ions to the coating. With higher metal-ion concentrations, the correspondingly doped fabrics left more residues. The T_p values of all of the coated fabrics shifted to lower temperatures compared to those of the control sample. The decrease in the flammability of all of the coated fabrics could be attributed to the phosphate groups released from the low-temperature decomposition of the coating; this promoted the charring of the fabric. The formation of a protective char barrier on the surface of the ramie fabric protected the underlying ramie from burning. What is more, when we compared the coated fabrics with the same coating components and BL numbers, the one with greater Zn content showed lower THR and HRC values but more residues; this was believed to be caused by the addition of Zn to the coating help accelerate the decomposition of the phosphorus-contained coating[22] and stabilize the char to further decrease the THR and HRC values.

All ramie fabrics were subjected to VFT to further evaluate their fire-retardant properties. All of the samples ignited immediately, but the spread speeds of the flame were quite different. The images of all of the fabrics at 5 s after ignition (Figure 11) showed that the flames of all of the coated fabrics spread much more slowly than that of the control and were also less vigorous. The flame was further weakened with more deposited BLs. The afterflame time for the control fabric was almost twice that of the coated fabrics (see Table IV). The long afterflame time of the control fabric was due to the fact that the burning process of the control fabric continued until the fabric was entirely consumed. However, for the coated fabrics, the flame-retardant coatings helped to diminish the decomposition of fabrics and led to an earlier end of the combustion process. As shown in Figure 12, the control fabric was entirely consumed after the burning process, whereas all of 15-BL coated fabrics left significant residues (see Figure S3 in the Supporting Information for images of the 5-BL and 10-BL coated fabrics). Those residues were still intact and were continuous.

The surface morphology of all of the coated fabrics before and after VFT were examined through SEM. To be comparable and representative, the samples were taken from the center of the residual char for those burned fabrics. Figure 13 presents the low-magnification SEM images of all of the 15-BL assembled coatings (see Figure S4 and S5 in the Supporting Information for images of the other fabrics). It was clear that the LbL assembly process did not alter the weave structure of the fabrics, and the coatings uniformly covered the surfaces of the fabrics. In addition, all of the coated fabrics retained the weave structure well, and the gaps between yarns only slightly increased after VFT. This was especially obvious for the fabric with 0.09*M* Zn-contained coating, whose residue morphology and structure were almost the same as those of the sample before burning. All of the coated fabrics showed a rough surface after burning, and there were clearly visible bubbles. The most obvious was the one with the 0.03*M* Zn-contained coating, whose surface was completely covered with a layer of char. This was further confirmed by high-magnification images. The gaps between fibers were full of bubbles, and the fibers were hidden under those shelters. All of these provided us with evidence that the addition of Cu and Zn to the PVPA-contained coating helped to impart better flame-retardant properties to the ramie fabric. The previous MCC and VFT results were in good accordance with those obtained in Grunlan et al.'s[17] and Alongi et al.'s[19] research; that is, phosphorus-containing flame retardants remarkably improved the flame retardancy of natural fibers. The additions of metal ions further improved the

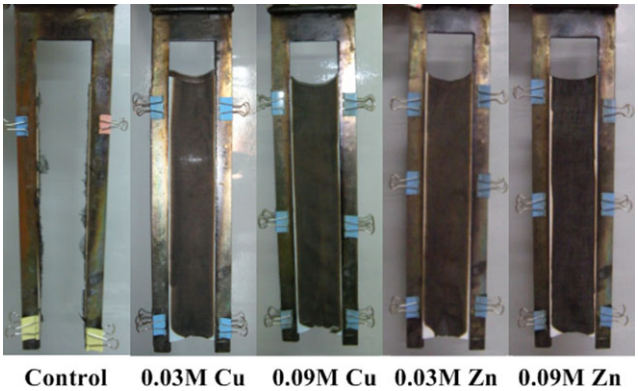

Figure 12. Images of the control and all of the 15-BL coated ramie fabrics after the VFT. [Color figure can be viewed in the online issue, which is available at wileyonlinelibrary.com.]

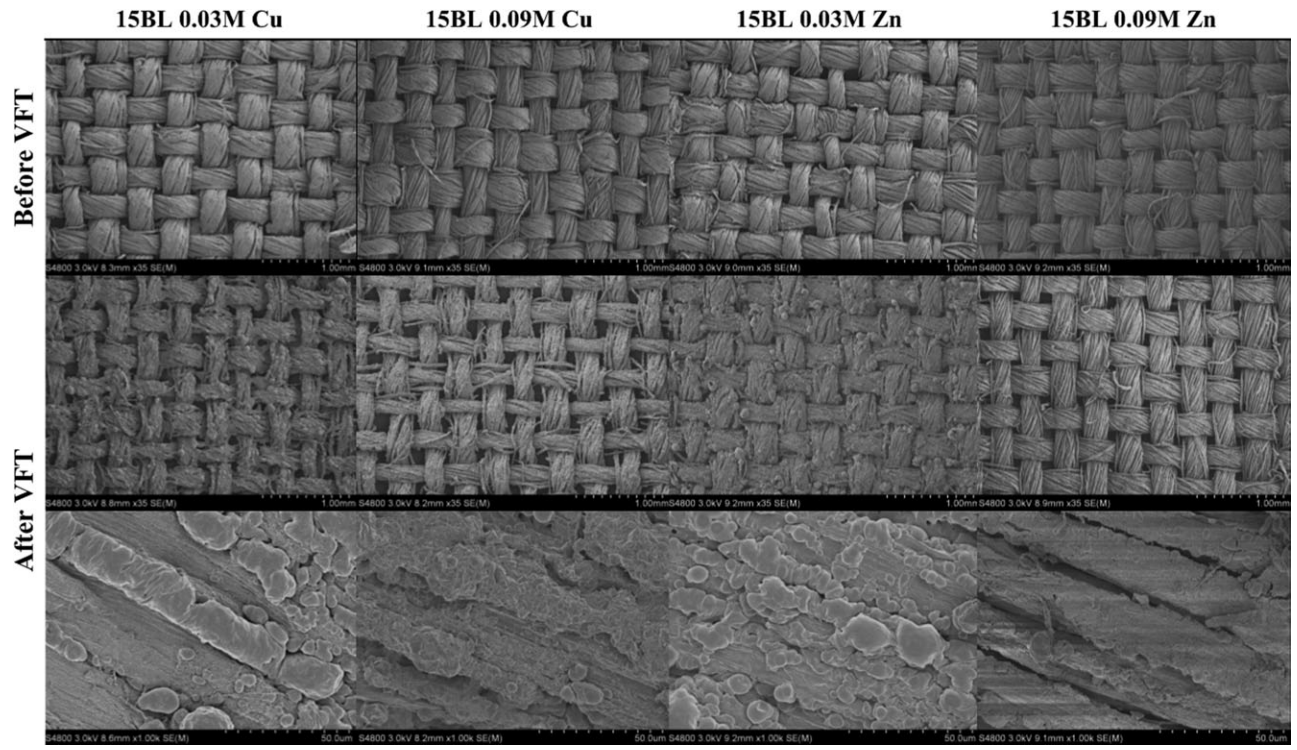

Figure 13. Low-magnification SEM images of all of the 15-BL coated ramie fabrics before and after the VFT. High-magnification SEM images of the corresponding residues are also shown.

flame-retardant efficiency of the phosphorus-containing flame retardants.

CONCLUSIONS

The surface modification of ramie fabrics with LbL-assembled Cu/Zn-ion-doped flame-retardant coatings dramatically improved the fire retardancy of fabrics. The coatings with well-distributed Cu/Zn ions homogeneously covered the surface of the ramie, acting as a protective shield upon heating and burning. The presence of Cu/Zn ions in coatings promoted the decomposition of flame-retardant components at lower temperatures, with an earlier release of phosphate groups from the decomposed flame retardant promoting the charring of the ramie fabric. This finally led to a remarkable improvement in the thermal and fire stability of the coated fabric. A significant residue, as much as 25.2 wt %, was left; this was nearly 30 times more than that of the control fabric. Moreover, the MCC results show that the coating greatly reduced THR by as much as 66% and HRC by 57%. The SEM images of the char after VFT revealed the particular advantage of Cu/Zn ions in protecting the original structure and morphology of the ramie fabric. Thus, these coatings could be promising for the flame-retardant modification of ramie fabrics and other materials, such as other natural textiles, polyester, and wood.

ACKNOWLEDGMENTS

The authors acknowledge financial support from the National Basic Research Program of China (contract grant number 2010CB631105).

REFERENCES

1. Horrocks, A. *R. Polym. Degrad. Stab.* **2011**, *96*, 377.
2. Decher, G.; Hong, J. D. *Makromol. Chem. Macromol. Symp.* **1991**, *46*, 321.
3. Mun, S.; Decker, E. A.; McClements, D. J. *J. Colloid Interface Sci.* **2006**, *296*, 581.
4. Zhang, H. Y.; Wang, D.; Wang, Z. Q.; Zhang, X. *Eur. Polym. J.* **2007**, *43*, 2784.
5. Choi, J. Y.; Rubner, M. F. *Macromolecules* **2005**, *38*, 116.
6. Yang, S. Y.; Rubner, M. F. *J. Am. Chem. Soc.* **2002**, *9*, 2100.
7. Ye, S. H.; Wang, C. Y.; Liu, X. X.; Tong, Z. *J. Controlled. Release.* **2005**, *106*, 319.
8. Dubas, S. T.; Schlenoff, J. B. *Macromolecules* **1999**, *32*, 8153.
9. Zeng, G. H.; Gao, J.; Chen, S. L.; Chen, H.; Wang, Z. Q.; Zhang, X. *Langmuir* **2007**, *23*, 11631.
10. Bai, S. L.; Wang, Z. Q.; Zhang, X. *Langmuir* **2004**, *20*, 11828.
11. Kohli, P.; Blanchard, G. *J. Langmuir* **2000**, *16*, 8518.
12. Kohli, P.; Blanchard, G. *J. Langmuir* **2000**, *16*, 4655.
13. Hatzor, A.; Boom-Moav, T.; Yochelis, S.; Vaskevich, A.; Shanzer, A.; Rubinstein, I. *Langmuir* **2000**, *16*, 4420.
14. Greenstein, M.; Ishay, R. B.; Maoz, B. M.; Leader, H.; Vaskevich, A.; Rubinstein, I. *Langmuir* **2010**, *26*, 7277.
15. Li, Y. C.; Schulz, J.; Grunlan, J. C. *Am. Chem. Soc. Appl. Mater. Interfaces* **2009**, *1*, 2338.

16. Li, Y. C.; Schulz, J.; Mannen, S.; Delhom, C.; Condon, B.; Chang, S. C.; Zammarano, M.; Grunlan, J. C. *Am. Chem. Soc. Nano.* **2010**, *4*, 3325.
17. Li, Y. C.; Mannen, S.; Morgan, A. B.; Chang, S. C.; Yang, Y. H.; Condon, B.; Grunlan, J. C. *Adv. Mater.* **2011**, *23*, 3926.
18. Carosio, F.; Alongi, J.; Malucelli, G. *Carbohydr. Polym.* **2012**, *88*, 1460.
19. Alongi, J.; Carosio, F.; Malucelli, G. *Cellulose* **2012**, *19*, 1041.
20. Yu, T.; Ren, J.; Li, S. M.; Yuan, H.; Li, Y. *Compos. A* **2010**, *41*, 499.
21. The Nightdress (Safety) Regulation, SI 839 and the Nightwear (Safety) Regulations SI 2043; HMSO: London, **1967** and 1985.
22. Gaan, S.; Sun, G. *J. Anal. Appl. Pyrolysis* **2007**, *78*, 371.
23. Tan, J.; Gemeinhart, R. A.; Ma, M.; Saltzman, W. M. *Biomaterials* **2005**, *26*, 3663.
24. Davies, P. J.; Horrocks,A. R.; Alderson,A. *Polym. Degrad. Stab.* **2005**, *88*, 114.
25. Lewin, M.; Endo, M. *Polym. Adv. Technol.* **2003**, *12*, 3.
26. Lam, Y. L.; Kan, C. W.; Yuen, C. W. M. *J. Appl. Polym. Sci.* **2011**, *121*, 267.
27. Hirschler, M. M. *Polymer.* **1984**, *25*, 405.
28. Cao, Z. H.; Zhang, Y.; Song, P. A.; Cai, Y. Z.; Guo, Q.; Fang, Z. P.; Peng, M. *J. Anal. Appl. Pyrolysis* **2011**, *92*, 339.
29. Xu, J.; Ding, G.; Li, J. L.; Yang, S. H.; Fang, B. S.; Sun, H. C.; Zhou, Y. M. *Appl. Surf. Sci.* **2010**, *256*, 7540.
30. Bingöl, B.; Meyer, W. H.; Wagner, M.; Wegner, G. *Macromol. Rapid Commun.* **2006**, *27*, 1719.
31. Le Bras, M.; Bourbigot, S.; Revel, B. *J. Mater. Sci.* **1999**, *34*, 5777.
32. Aslan, A.; Bozkurt, A. *J. Power Sources* **2012**, *217*, 158.
33. Kavlak, S.; Güner, A.; Rzayev, Z. M. O. *J. Appl. Polym. Sci.* **2012**, *125*, 3617.
34. Cao, W. M.; Wang, J. B.; Wang, Y. L. *Langmuir* **2007**, *23*, 3142.
35. Wang, S. R.; Liu, Q.; Luo, Z. Y.; Wen, L. H.; Cen, K. F. *Front. Energy Power. Eng. China* **2007**, *1*, 413.
36. Yang, Z.; Wang, X.; Lei, D.; Fei, B.; Xin, J. *H. Polym. Degrad. Stab.* **2012**, *97*, 2467.
37. Jiang, D. D.; Yao, Q.; McKinney, M. A.; Wilkie, C. A. *Polym. Degrad. Stab.* **1999**, *63*, 423.
38. Nedel'ko, V. V.; Korsunskii, B. L.; Dubovitskii, F. I.; Gromova, G. L. *Polym. Sci. USSR* **1975**, *17*, 1697.